

## Tuning the structure of 1,3,5-benzene tricarboxamide self-assemblies through stereochemistry

*Xavier Caumes, Arianna Baldi, Geoffrey Gontard, Patrick Brocorens, Roberto Lazzaroni, Nicolas Vanthuyne, Claire Troufflard, Matthieu Raynal and Laurent Bouteiller*

### SUPPORTING INFORMATION

#### General Procedures.

Preparation of new compounds: Synthetic procedures for the preparation of **BTA (S)-Cha<sup>t</sup>-Pr** and **BTA (S)-Cha<sup>t</sup>-Bu** are detailed in page S21-S22. (S)-(+)- $\alpha$ -aminocyclohexanepropionic acid hydrate was purchased from Sigma-Aldrich (technical grade) and used as received. All other reagents were purchased from commercial sources and were used directly. **BTA (S)-Val** and **BTA (rac)-Val** were prepared following published procedures.<sup>1</sup> **Model BTA** was prepared by reacting benzoyl chloride and the dodecyl ester of L-Norleucine in dichloromethane. Chiral HPLC analyses showed that **BTA (S)-Val** was optically pure ( $ee > 99\%$ ,  $de > 99\%$ ) and that **BTA (rac)-Val** contains the four stereoisomers, **BTA (S,S,R)-Val** (37.5%), **BTA (R,R,S)-Val** (37.5%), **BTA (S)-Val** (12.5%) and **BTA (R)-Val** (12.5%) in the expected proportions for a statistical distribution of then enantiomers during the reaction between trimesoyl chloride and a racemic mixture of the dodecyl ester of valine. **BTA (S,S,R)-Val** was isolated from **BTA (rac)-Val** thanks to preparative chiral HPLC (see analytical details in page S23,  $ee > 99\%$ ,  $de > 99\%$ ). Unless otherwise noted, chromatography-grade solvents were used as received. Dried solvents were obtained from an SPS solvent purification system (IT-Inc) and stored on 4 Å molecular sieves. Triethylamine was dried by distillation over CaH<sub>2</sub> and stored over 4 Å molecular sieves. All inert atmosphere reactions were carried out under an argon atmosphere with standard Schlenk-line techniques. NMR spectra were recorded on a Bruker Avance 300 or on a Bruker Avance 600 spectrometer and calibrated to the residual solvent peak: DMSO-d<sub>6</sub> (<sup>1</sup>H: 2.50 ppm; <sup>13</sup>C: 39.52 ppm) and acetone-d<sub>6</sub> (<sup>1</sup>H: 2.05 ppm; <sup>13</sup>C: 29.84 ppm). Peaks are reported with their corresponding multiplicity (s: singlet; d: doublet, t: triplet; hept: heptuplet) and integration, and respective *J* coupling constants are given in Hertz. Exact mass measurements (HRMS) were obtained on TQ R30-10 HRMS spectrometer by ESI+ ionization and are reported in *m/z* for the major signal.

Preparation of BTA solutions for analyses: the desired BTA was weighed into a ø11.6 mm HPLC vial or a ø20 mm glass vial, the volume of solvent (cyclohexane or methylcyclohexane) was adjusted to the desired end concentration with an adequate glass microsyringe, and verified by weighing the sample. Vials were sealed with PTFE-coated caps to avoid contamination from leaching plasticizer. All BTAs dissolve at rt after a few hours on a shaking table (250 rpm). 13 wt% cyclohexane solutions (Fig. 4) were heated to 50°C in order to get homogeneous viscous solutions or gels. The gels showed no syneresis even after 1 month at rt.

Viscosimetry: viscosimetry measurements were performed with a Cannon-Manning Semi-Micro U-tube viscosimeter (size 100) immersed in a thermostated water bath (20 °C). Viscosity values are reported as an average of 2 measurements and normalized by that of cyclohexane measured at the same temperature (Fig. 4).

Fourier-Transform Infrared (FT-IR) analyses: FT-IR measurements were performed on a Nicolet iS10 spectrometer. FT-IR spectra of the solids (thin film) were recorded by reflection on a Ge probe (ATR-FTIR). Spectra of cyclohexane solutions were measured in CaF<sub>2</sub> cells at 20 °C by adjusting the pathlength to the concentration: 0.01 cm (90 mM), 0.05 cm (10 mM, 15 mM, 20 mM, 30 mM) and 0.1 cm (2 mM) and were corrected for air, cyclohexane and cell absorption.

Small-angle neutron scattering (SANS) analyses: SANS measurements were made at the LLB (Saclay, France) on the PA20 instrument, at two distance-wavelength combinations to cover the  $4.2 \times 10^{-3}$  to  $0.25 \text{ \AA}^{-1}$   $q$ -range, where the scattering vector  $q$  is defined as usual, assuming elastic scattering, as  $q = (4\pi/\lambda)\sin(\theta/2)$ , where  $\theta$  is the angle between incident and scattered beam. Data were corrected for the empty cell signal and the solute and solvent incoherent background. A light water standard was used to normalize the scattered intensities to  $\text{cm}^{-1}$  units.

X-ray analyses: see page S24.

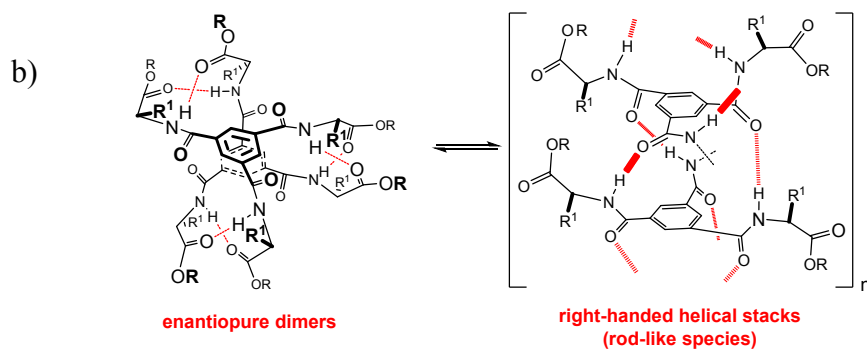
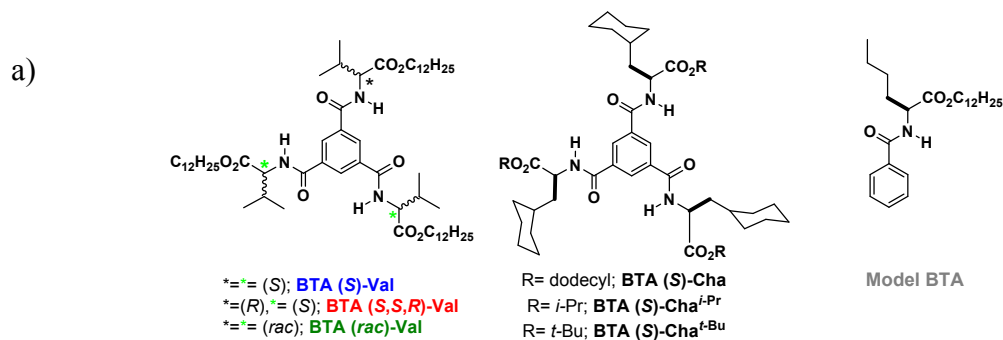
Circular dichroism (CD) analyses: CD measurements were performed on a Jasco J-1500 spectrometer equipped with a Peltier thermostated cell holder and Xe laser (lamp XBO 150W/4). Data were recorded at 20°C (unless otherwise stated) with the following parameters: 20  $\text{nm} \cdot \text{min}^{-1}$  sweep rate, 0.05 nm data pitch, 2.0 nm bandwidth, and between 300 and 200 nm. Solvent (cyclohexane or methylcyclohexane) and cell contributions at the same temperature were subtracted from the obtained signals. The pathlength of the quartz cell was adapted to the concentration: 0.1 mm dismountable quartz cell (2 mM) and 5 mm closed quartz cell (25  $\mu\text{M}$ ). Molar CD values are reported in  $\text{L} \cdot \text{mol}^{-1} \cdot \text{cm}^{-1}$  and are expressed as follows:  $\Delta\epsilon = \theta / (32980 \times l \times c)$  where  $\theta$  is the measured ellipticity (mdeg),  $l$  is the optical pathlength in cm, and  $c$  is the concentration in  $\text{mol} \cdot \text{L}^{-1}$ . For VT-CD experiments, the temperature was controlled with a Peltier thermostated cell holder and the pathlength was adapted to the concentration (5 mm). Heating rate was set to  $1^\circ\text{C} \cdot \text{min}^{-1}$  and spectra were recorded every  $10^\circ\text{C}$  between  $-5^\circ\text{C}$  and  $117^\circ\text{C}$ . For all samples, LD contribution was negligible ( $\Delta\text{LD} < 0.005$  dOD) and the shape of the CD signal was independent of the orientation of the quartz slide.

UV-Vis analyses: UV-Vis absorption spectra were extracted from CD on each of the above samples and obtained after correction of the absorption of air, solvent (cyclohexane or methylcyclohexane), and cell at the same temperature.

Molecular modelling: Dimers of **BTA (S)-Val** and **BTA (S,S,R)-Val** (structure I-III) were built and modelled with the Materials Studio 6.0 modelling package from Accelrys (now Biovia). The dodecyl ester groups were replaced by methyl ester groups to alleviate the computational cost. As a forcefield, Dreiding<sup>2</sup> was used, with charges on the atoms assigned from the polymer consistent force field (PCFF),<sup>3, 4</sup> and a long-range interaction cutoff set to 14 Å with a spline width of 3 Å. The dielectric constant was distance-dependent. The dimers were first submitted to molecular mechanics (MM) energy minimizations using a conjugate gradient algorithm until a convergence criterion of 0.001 kcal per  $\text{mol} \cdot \text{Å}$  was reached. MD simulations were then performed in the canonical (N,V,T) ensemble. The Nose<sup>5</sup> thermal bath coupling was used to maintain the temperature at 298 K, with a coupling constant of 0.01, and the Verlet

velocity algorithm was used to integrate the equations of motion during 10 ns, with a 1-fs time step. The analyses were performed on the structures generated during the last 9 ns of the simulation.

NMR analyses: NMR experiments were recorded on a Bruker Avance III 600 spectrometer (14.1T) equipped with a BBO probe with z-axis gradient coil with maximum gradient strength of 55.4 G/cm. All spectra were acquired in 5 mm NMR tubes. Each NMR tube contained 10 mM of ester BTAs in cyclohexane-d<sub>12</sub> (<sup>1</sup>H, 1.38 ppm) or acetone-d<sub>6</sub> (<sup>1</sup>H, 2.05 ppm). 2D-homonuclear experiments (COSY and ROESY) were performed on **BTA (S)-Cha<sup>i</sup>-Pr** and **BTA (S)-Val**.



(a) Chemical structures of the BTAs investigated in this study. (b) Molecular structures of the enantiopure rod-like and dimeric hydrogen-bonded species formed by BTAs derived from (*S*)  $\alpha$ -amino esters.<sup>6, 7</sup> **Model BTA** was prepared to provide a diagnostic characterization of the monomeric form in FT-IR spectroscopy.

## Supplementary figures.

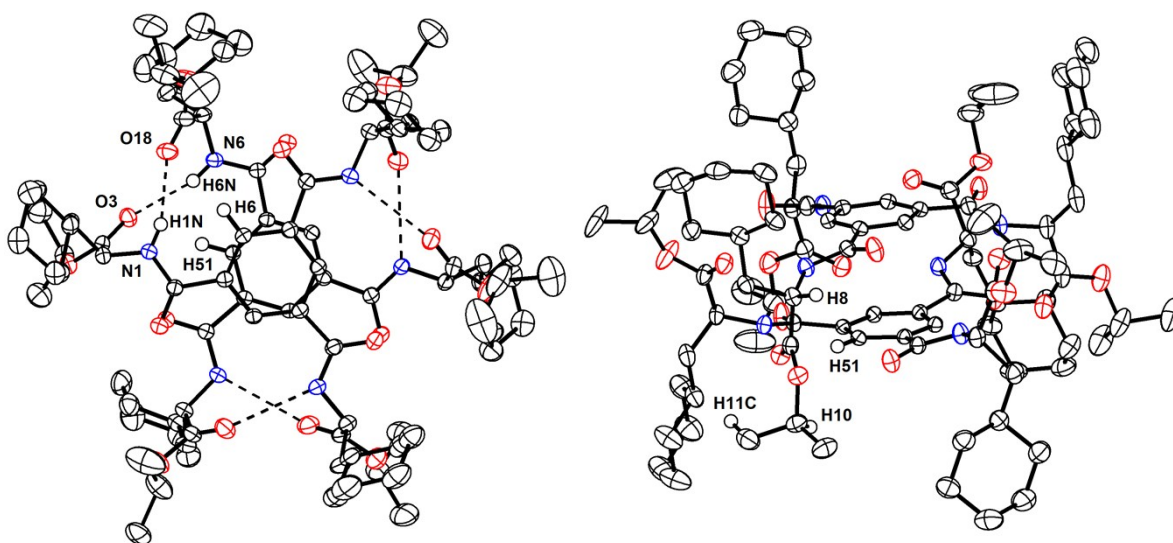


**Figure S1.** X-ray crystal structure of BTA (*S*)-Cha<sup>i</sup>-Pr·0.25CH<sub>3</sub>CN·0.5H<sub>2</sub>O in top view (left) and side view (right). Hydrogen atoms (except H1N, H6N, H6, H51, H8, H10, H11C) and solvent molecules are omitted for clarity. Ellipsoids are represented at 30% probability level. Selected distances (Å): H1N-O18: 2.159(3); H6N-O3: 2.204(3); H6-O18: 2.482(2); H51-O3: 2.352(3); H51-H8: 4.337(4); H51-H10: 3.489(4); H51-H11C: 4.674(4).

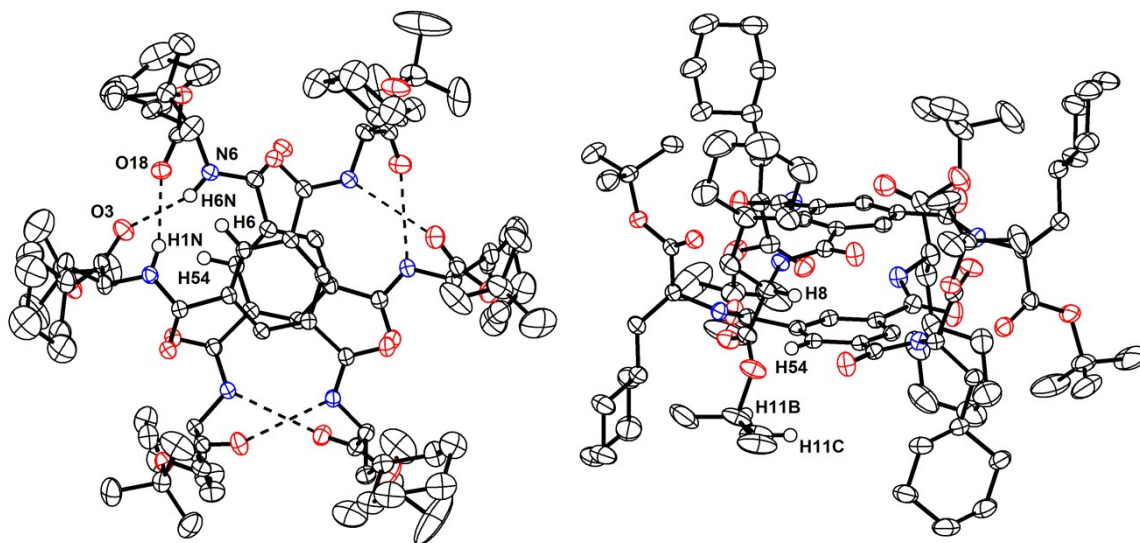


**Figure S2.** X-ray crystal structure of BTA (*S*)-Cha<sup>t</sup>-Bu in top view (left) and side view (right). Hydrogen atoms (except H1N, H6N, H6, H54, H8, H11B, H11C) are omitted for clarity. Ellipsoids are represented at 30% probability level. Selected distances (Å): H1N-O18: 2.187(3); H6N-O3: 2.166(3); H6-O18: 2.383(3); H54-O3: 2.526(2); H54-H8: 4.135(4); H54-H11B: 2.683(3); H54-H11C: 3.285(4).

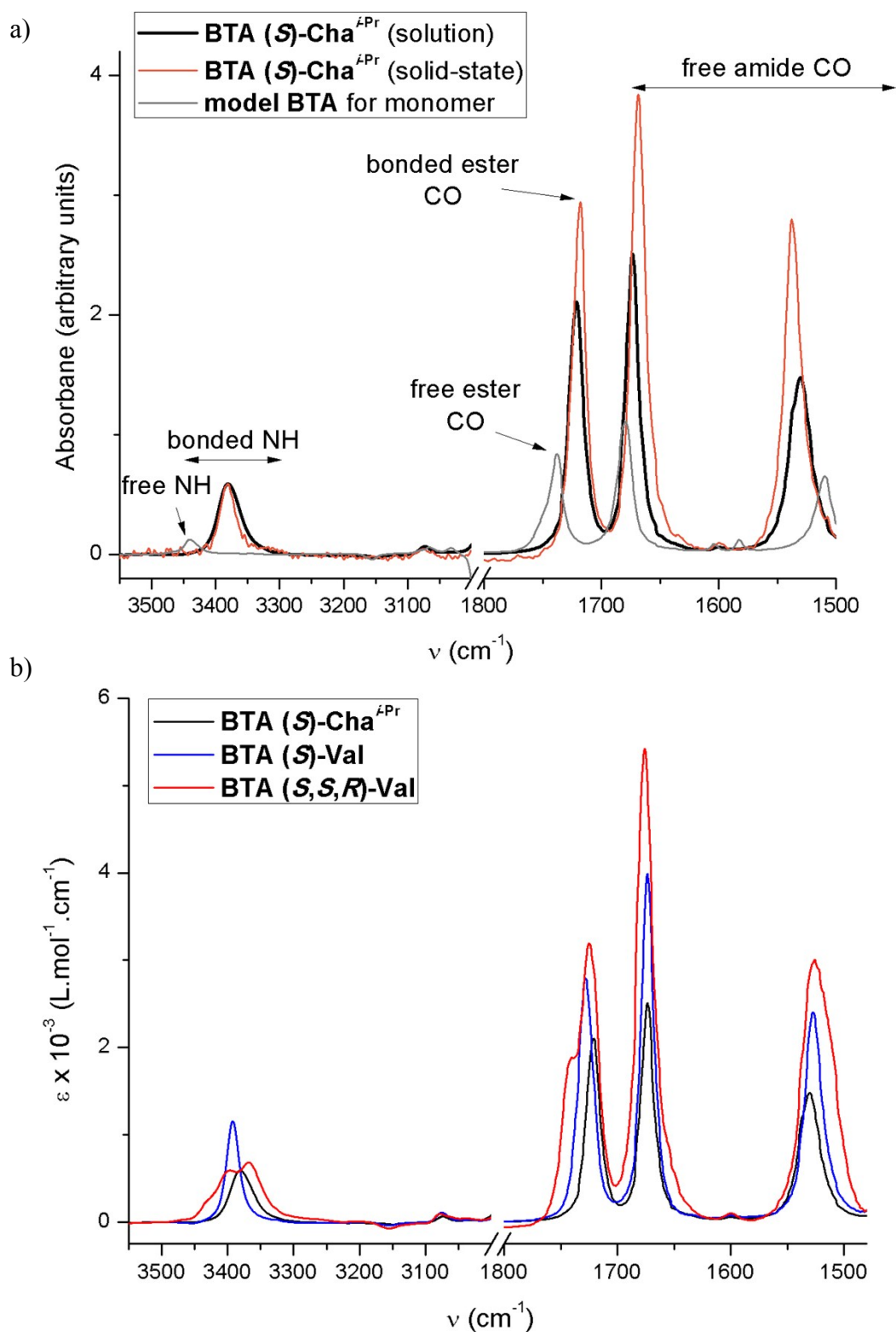


**Figure S3.** (a) FT-IR spectra of **BTA (S)-Cha<sup>iPr</sup>** in the solid-state and in cyclohexane (10 mM) and of **model BTA** in cyclohexane (10 mM) at 20 °C. (b) FT-IR spectra of **BTA (S)-Cha<sup>iPr</sup>**, of **BTA (S)-Val** and of **BTA (S,S,R)-Val** in cyclohexane (10 mM) at 20 °C. FT-IR analyses of **BTA (S)-Cha<sup>iPr</sup>** (solid-state and solution) and of **BTA (S)-Val** (solution) show frequencies diagnostic of ester-bonded dimers whilst **model BTA** exhibit frequencies characteristic of free N-H and C=O functions.

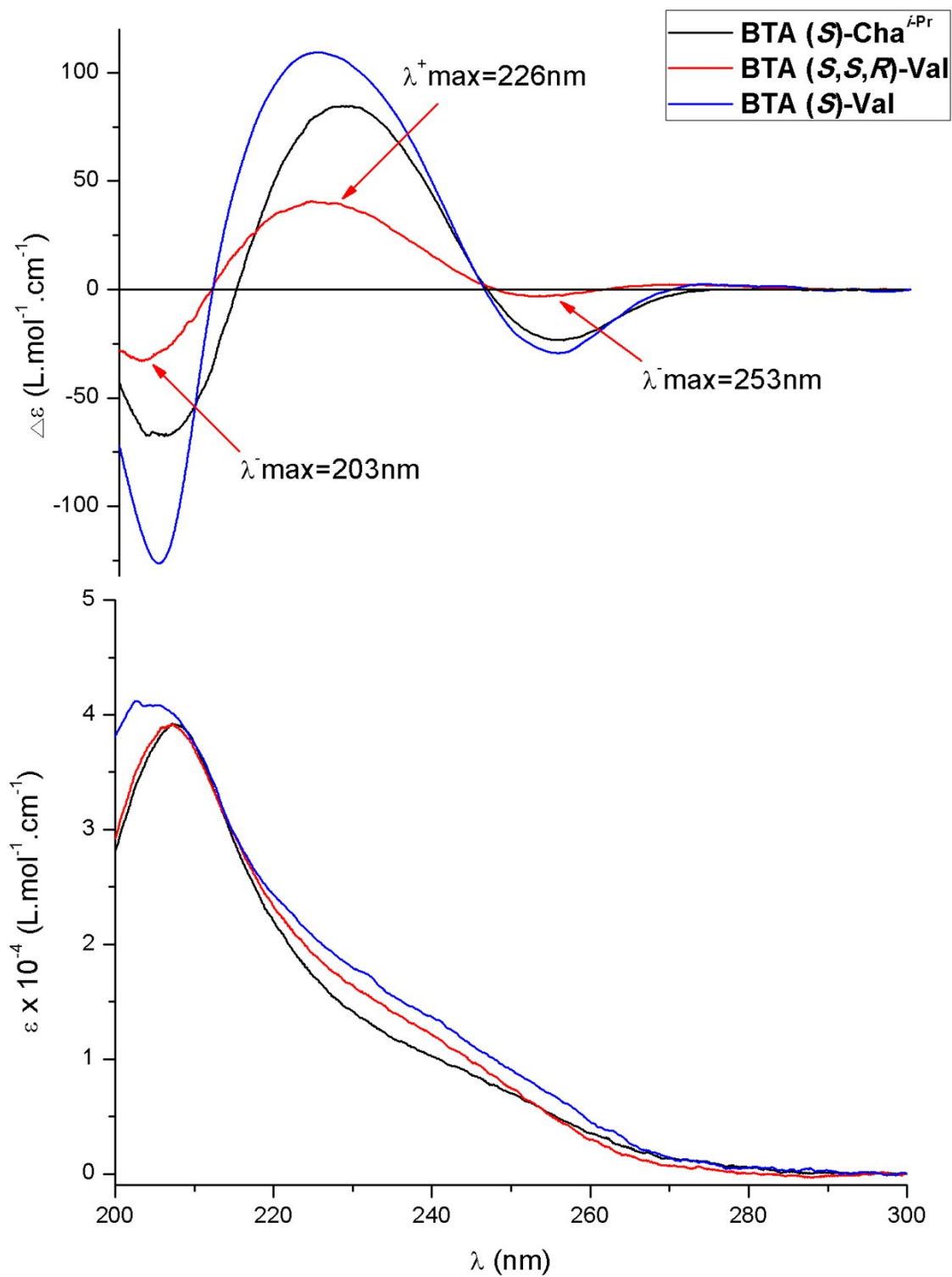
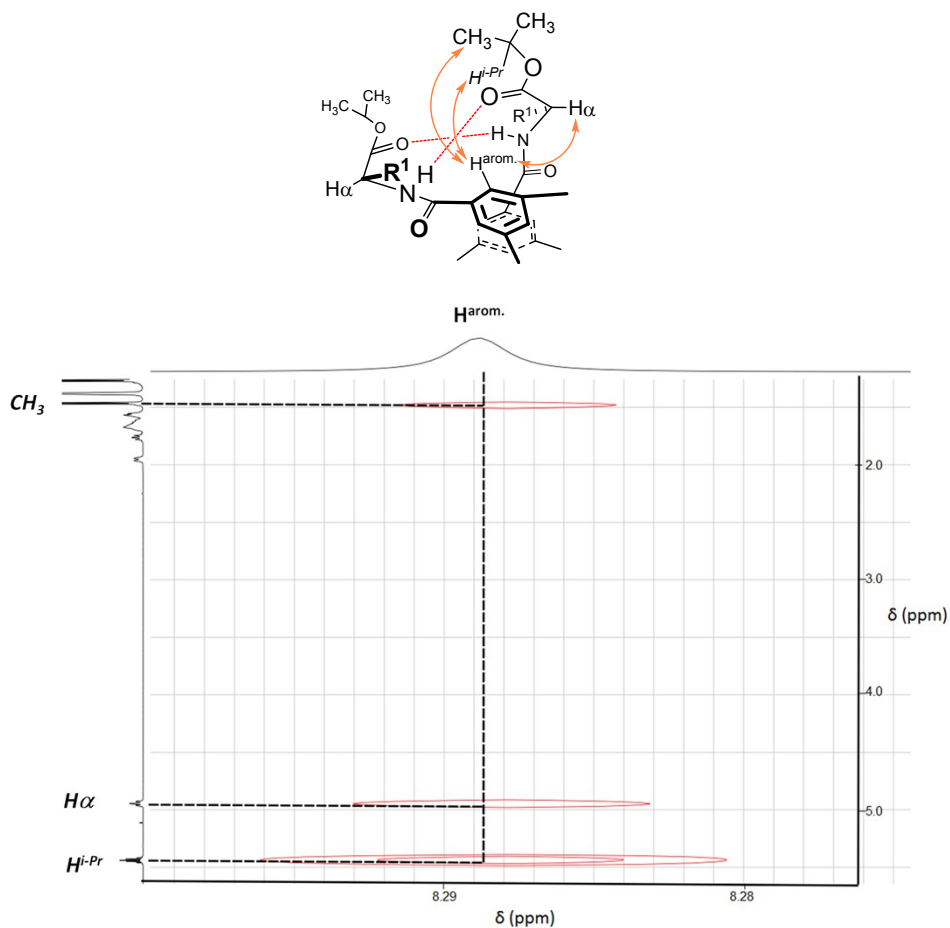


**Figure S4.** CD (top) and UV (bottom) spectra of **BTA (S)-Cha<sup>i</sup>Pr** of **BTA (S)-Val** and of **BTA (S,S,R)-Val** in cyclohexane (2 mM) at 20°C.



a)



b)

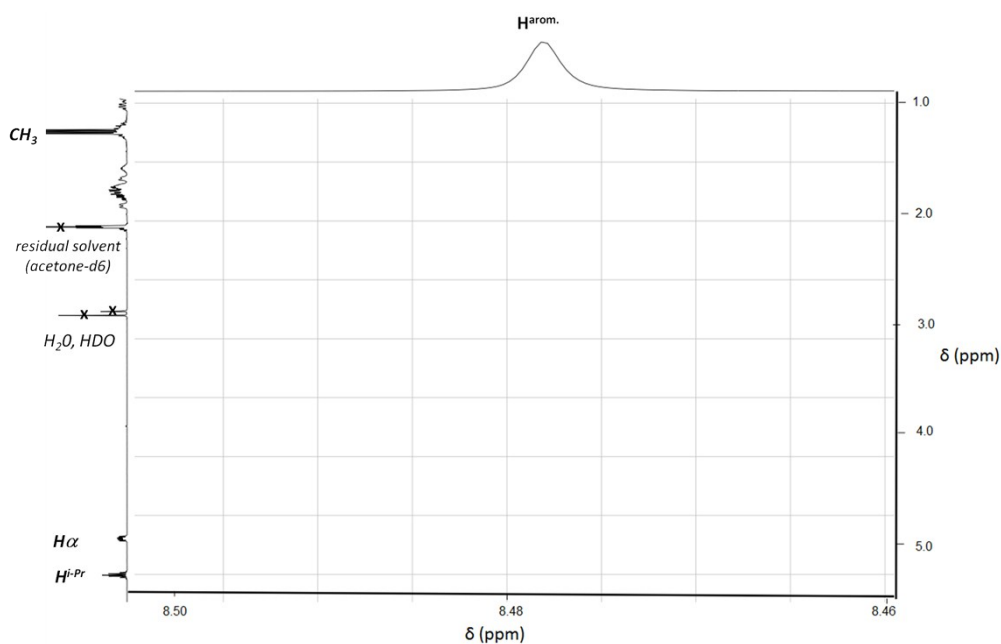


**Figure S6.** ROESY analyses of BTA (*S*)-Cha<sup>i-Pr</sup> in (a) C<sub>6</sub>D<sub>12</sub> (10 mM, dimers) and (b) acetone-d<sub>6</sub> (10 mM, monomers). Region showing the dipolar couplings between the aromatic C-H protons (denoted as H<sup>arom.</sup>, all equivalent) and: i) the methyne proton of the  $\alpha$ -carbon ( $H_{\alpha}$ ), ii) the methyne proton of the *i*-Pr group ( $H^{i-Pr}$ ), and iii) one methyl group of the *i*-Pr moiety ( $CH_3$ ). The NOE contacts, shown as orange arrows in the schematic representation, are characteristic of the dimer since these NOE contacts are not present in the monomer (b).

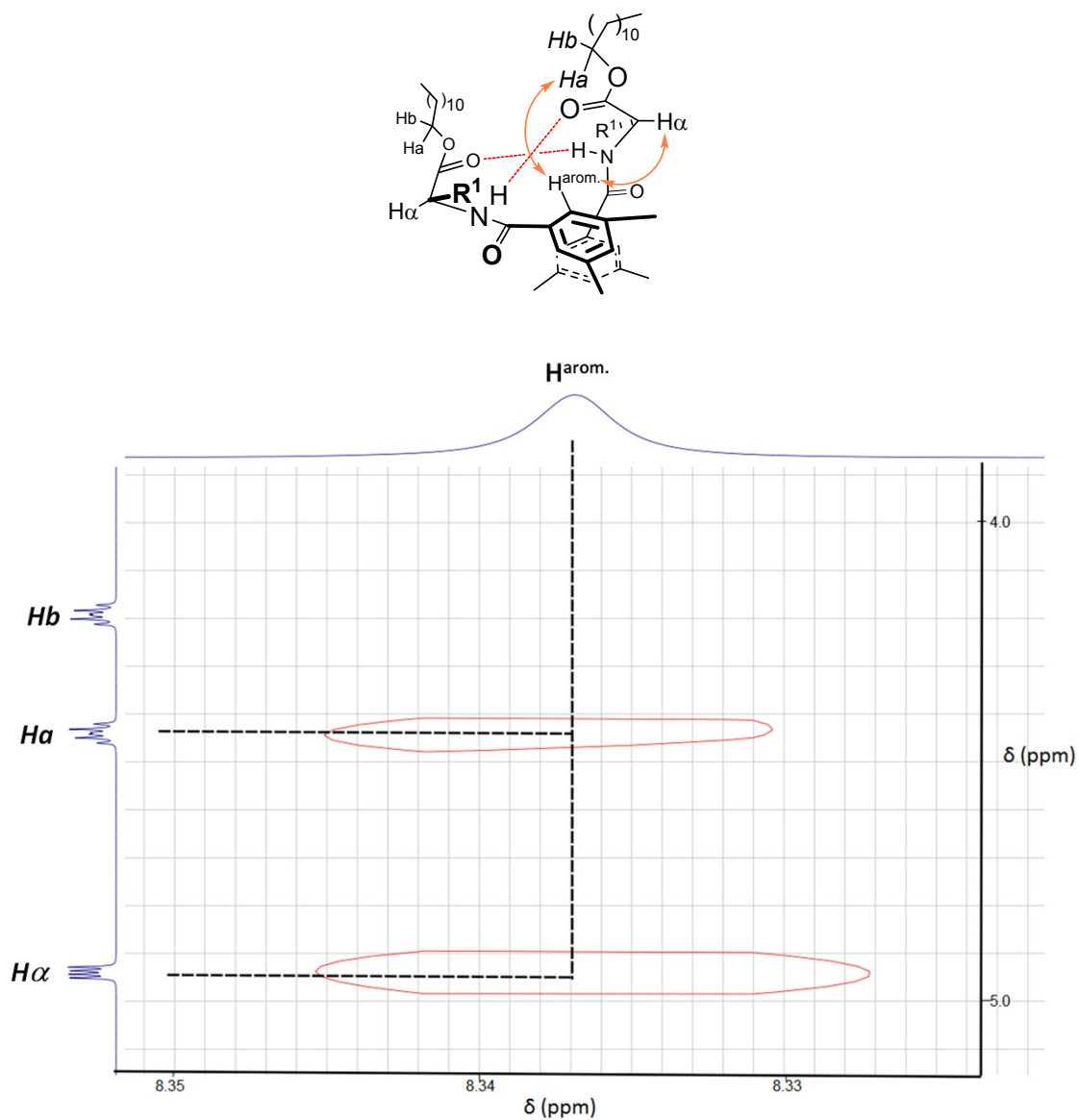


**Figure S7.** ROESY analyses of **BTA (S)-Val** in  $C_6D_{12}$  (10 mM). Region showing the dipolar couplings between the aromatic C-H protons (denoted as  $H^{arom.}$ , all equivalent) and: i) the methyne proton of the  $\alpha$ -carbon ( $H\alpha$ ), and ii) one of the  $Ha/Hb$  diastereotopic protons. These NOE contacts are shown as orange arrows in the schematic representation of the dimer.

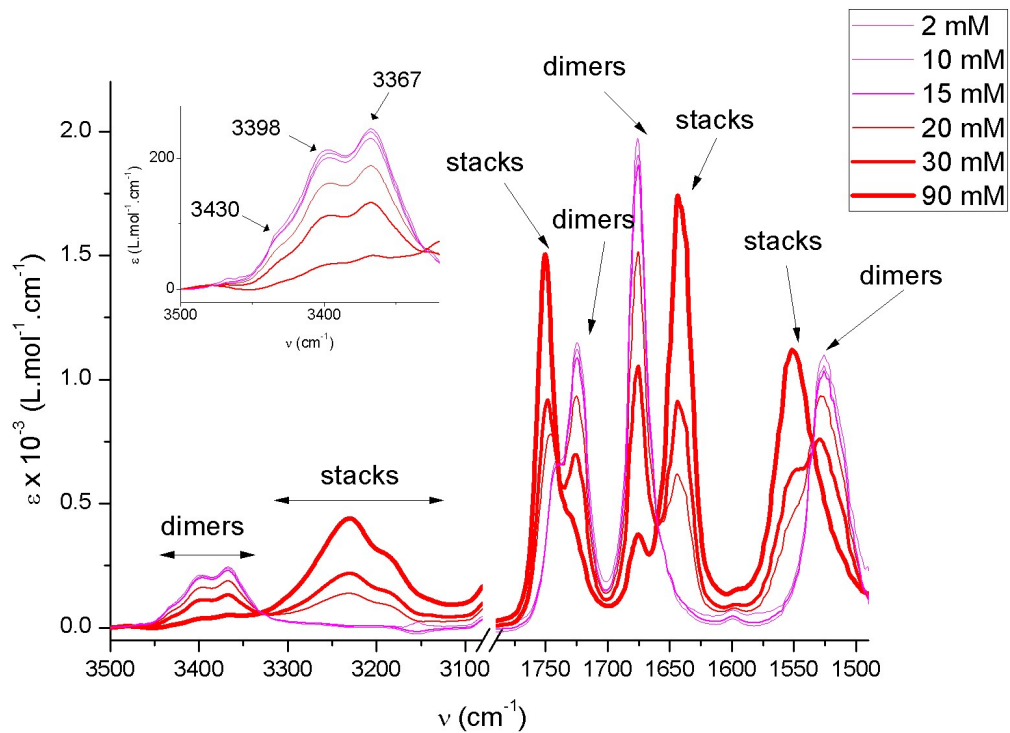


**Figure S8.** FT-IR spectra of **BTA (*S,S,R*)-Val** at various concentrations (2-90 mM) in cyclohexane at 20°C. Zoom on the N-H (left) and C=O (right) regions. Inset: zoom on the N-H absorption bands related to the hydrogen-bonded dimers.

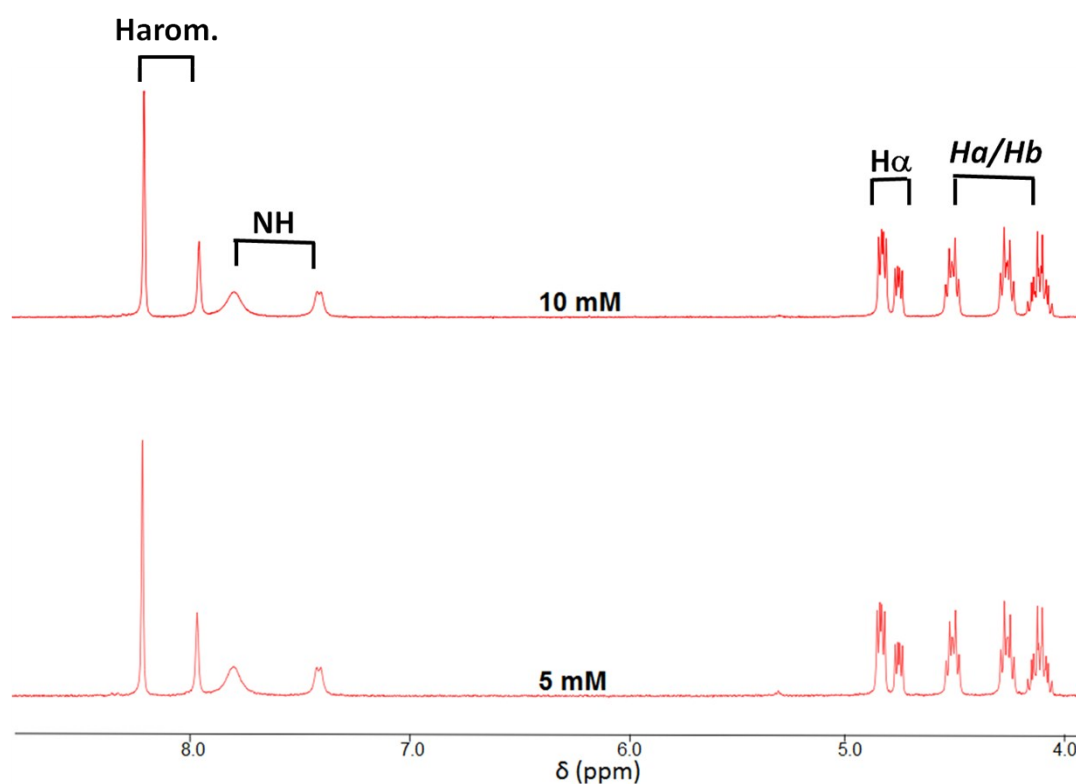
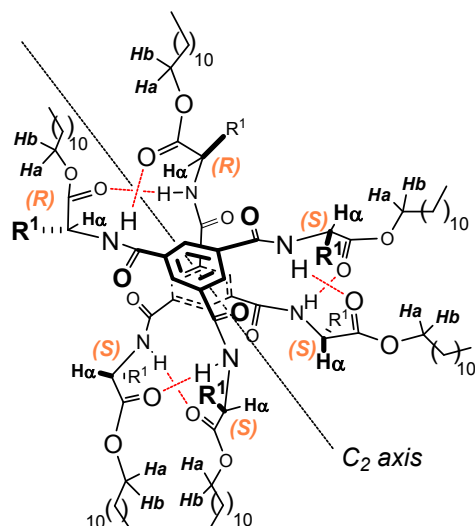
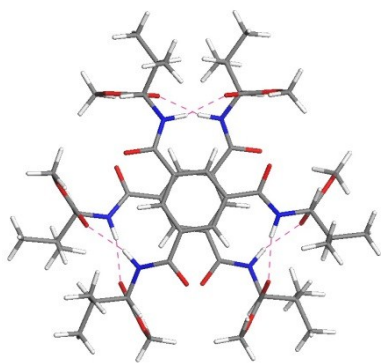
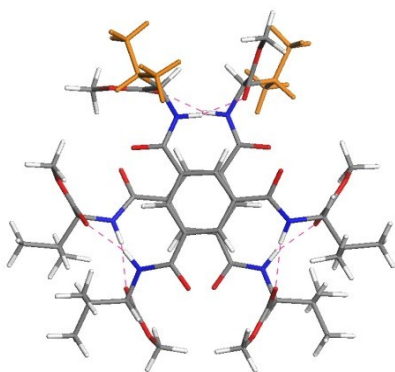
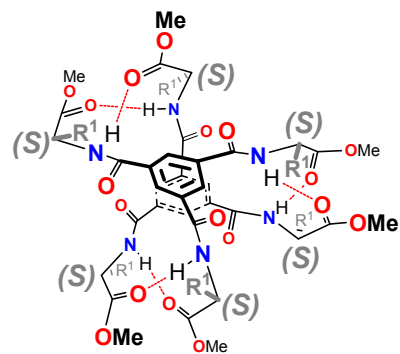


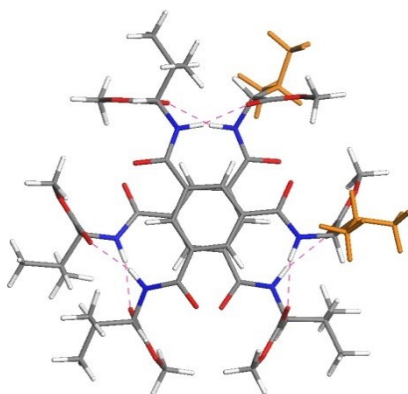
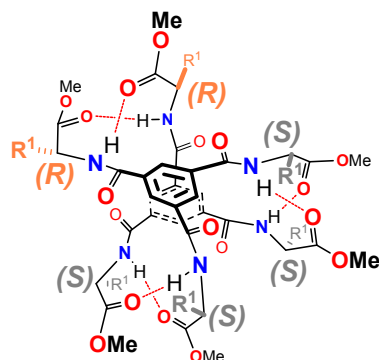
**Figure S9.**  $^1\text{H}$  NMR spectra of **BTA (S,S,R)-Val** in  $\text{C}_6\text{D}_{12}$  at 5 mM and 10 mM at  $20^\circ\text{C}$ . Zoom on the region between 4.0 and 8.8 ppm. Signals in this region correspond to the aromatic C-H hydrogens (denoted as H arom., two inequivalent singlets), the N-H protons (two inequivalent signals),  $\text{H}_\alpha$  (two inequivalent multiplets), and  $\text{H}_a/\text{H}_b$  (three inequivalent multiplets) of the dimers according to the labelling shown in the schematic representation of the dimers of **BTA (S,S,R)-Val** (structure I took as an example).



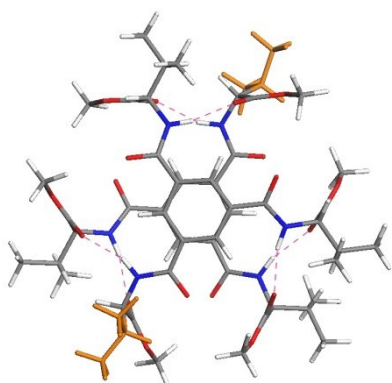
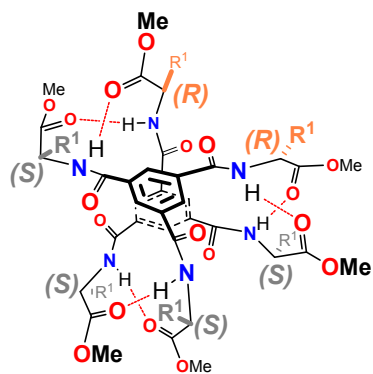
BTA (*S*)-Val<sup>Me</sup>



BTA (*S,S,R*)-Val<sup>Me</sup> structure I



BTA (*S,S,R*)-Val<sup>Me</sup> structure II



BTA (*S,S,R*)-Val<sup>Me</sup> structure III

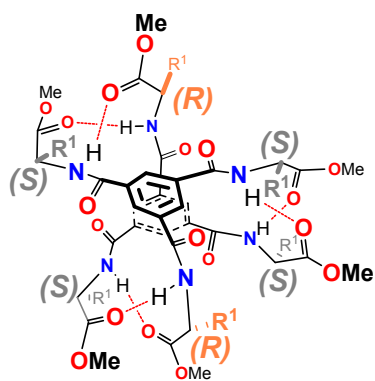


**Figure S10.** Energy-minimized structures of BTA (*S*)-Val<sup>Me</sup> and of BTA (*S,S,R*)-Val<sup>Me</sup> (structures I-III). R<sup>1</sup>= *i*-Pr. The *i*-Pr groups attached to a (*R*) stereogenic carbon are shown in orange.

**Table S1.** Relative total potential, hydrogen-bond, valence and non-bonding energies of the structures I-III of **BTA (S,S,R)-Val<sup>Me</sup>** with respect to **BTA (S)-Val<sup>Me</sup>**; average from the MD.

Relative energy with respect to <b>BTA (S)-Val<sup>Me</sup></b> (kcal/mol)	Total potential energy	Hydrogen bond energy	Valence Energy	Non-bonding energy
<b>BTA (S,S,R)-Val<sup>Me</sup> I</b>	5.2	0.5	5.5	-0.8
<b>BTA (S,S,R)-Val<sup>Me</sup> II</b>	5.7	1.1	3.7	0.9
<b>BTA (S,S,R)-Val<sup>Me</sup> III</b>	5.3	1.4	4.2	-0.3

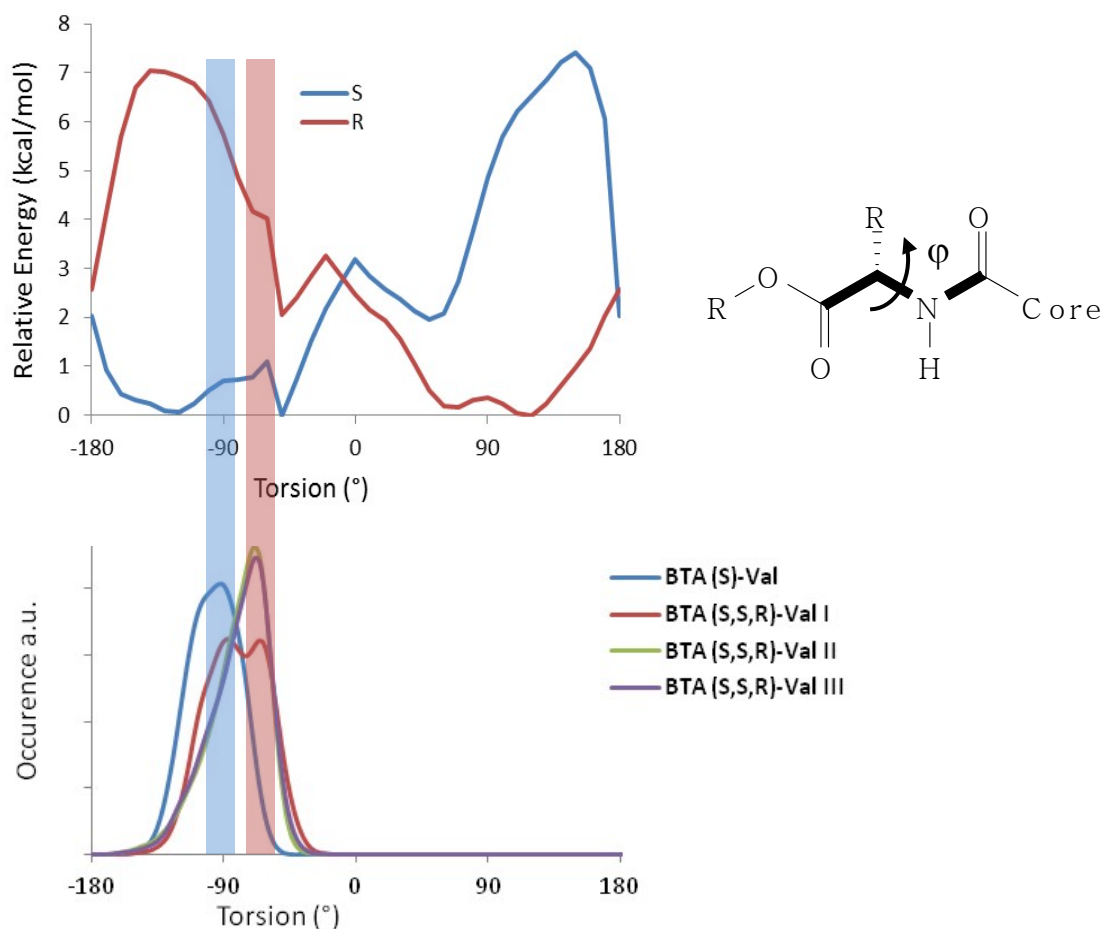


**Figure S11.** Top: evolution of the potential energy of an isolated BTA branch in function of the torsion  $\phi$ ; results for *R* and *S* branches (as an approximation for the calculation,  $R=CH_3$  and the core is H). Bottom: values of  $\phi$  adopted by the branches in the BTA dimers during the MD. In a (*P*) diastereomer of BTA, hydrogen bonds occur when  $\phi$  is about  $-90^\circ$ . This torsion value corresponds to a low energy region for *S* branches, and to a high energy region for *R* branches, which relax somewhat by increasing their torsion to about  $-60^\circ$ . The relaxation, however, is small to maintain the H bonds, which explains the origin of the destabilization of **BTA (S,S,R)-Val** with respect to **BTA (S)-Val**.

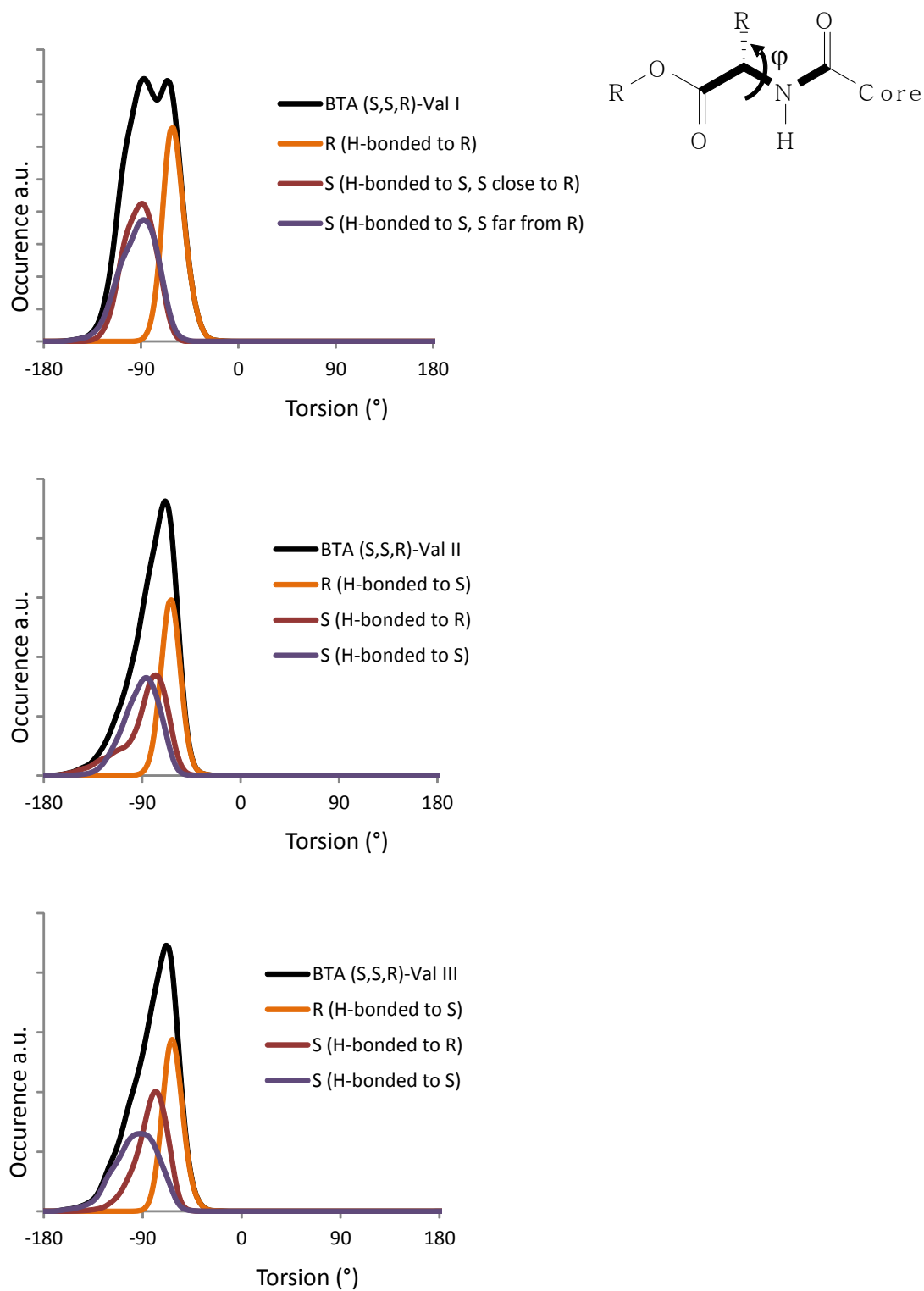


**Figure S12.** Values of  $\phi$  adopted by the branches in the **BTA (*S,S,R*)-Val<sup>Me</sup>** dimers during the MD. Decomposition of the total signal in function of the nature of the branch (*R* or *S*) and of its neighbors.

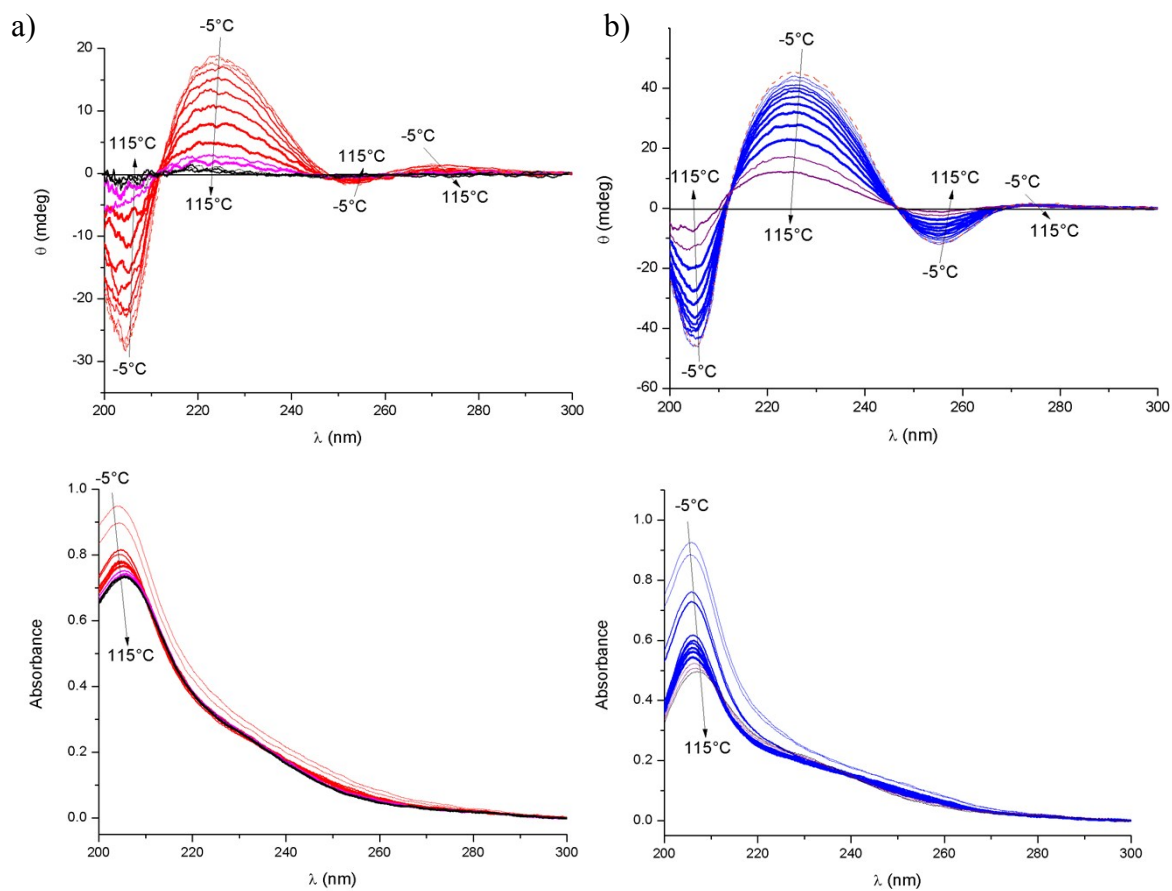


**Figure S13.** Transition between dimers and monomers for **BTA (*S,S,R*)-Val** (a) and **BTA (*S*)-Val** (b) probed by CD (top) and UV (bottom) experiments between -5°C and 115°C in methylcyclohexane ( $c=25 \mu\text{M}$ ). Heating rate:  $1^\circ\text{C}\cdot\text{min}^{-1}$ , spectra recorded every  $10^\circ\text{C}$ . These experiments have been performed in a closed quartz cell which explain why some of the measured temperatures exceed the boiling point of methylcyclohexane. Spectra in dashed red lines correspond to spectra obtained upon returning to the initial temperature (-5°C).

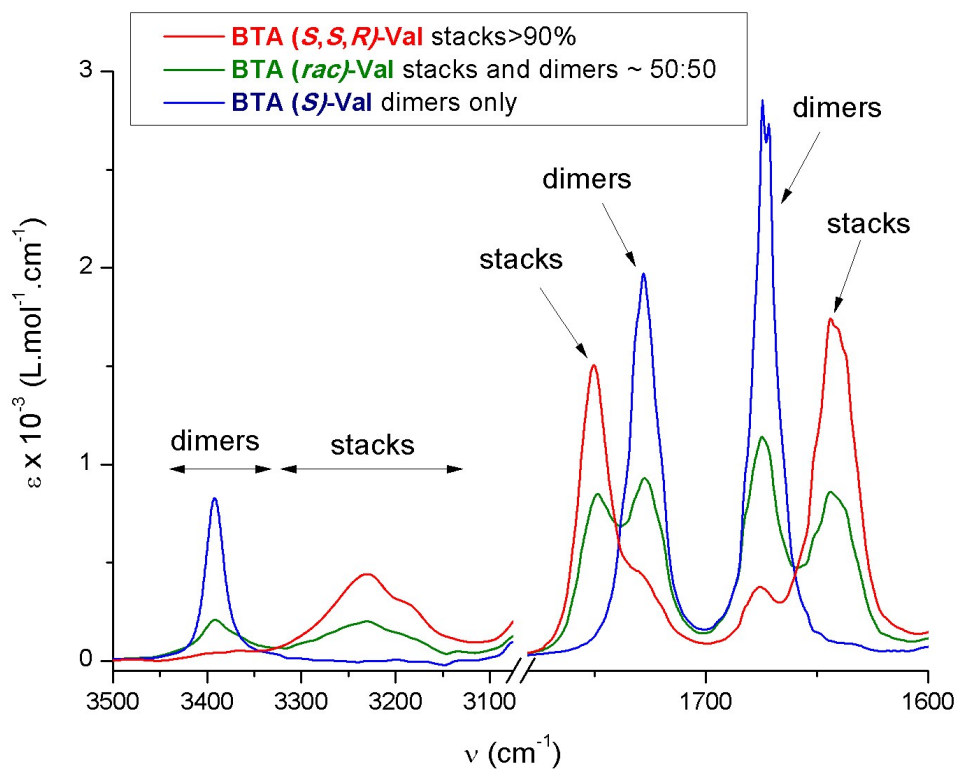


**Figure S14.** FT-IR spectra of **BTA (S,S,R)-Val**, **BTA (rac)-Val** and **BTA (S)-Val** in cyclohexane (90 mM) at 20°C. Zoom on the N-H (left) and C=O (right) regions.

The respective percentage of dimers and stacks for **BTA (rac)-Val** and **BTA (S,S,R)-Val** is estimated according to the relative intensity of the ester C=O absorption bands.

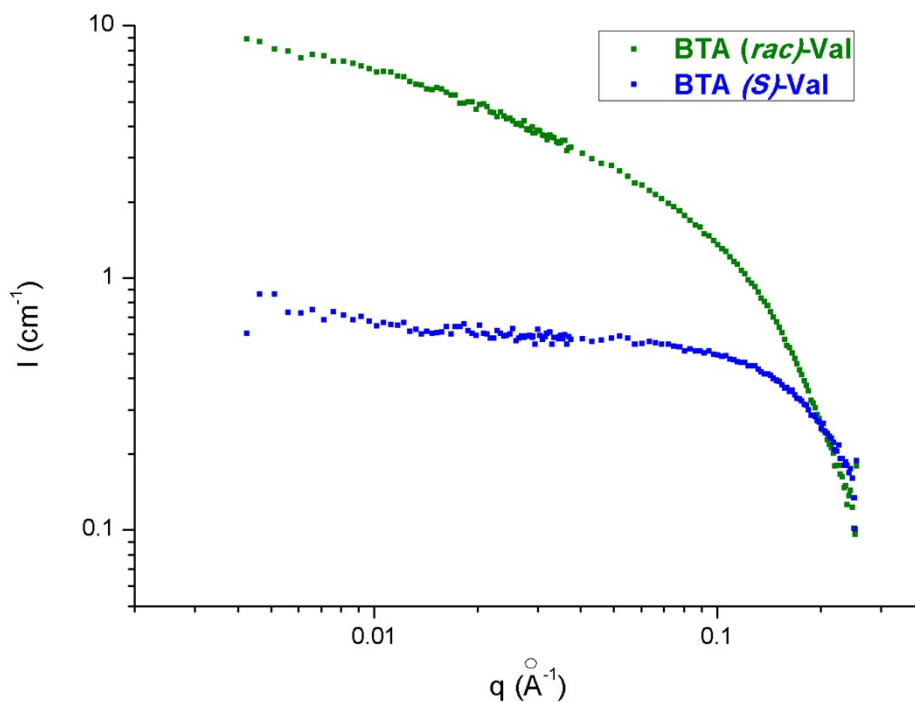
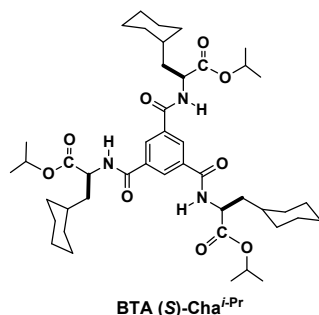


**Figure S15.** Characterisation by SANS of the assemblies formed by **BTA (*rac*)-Val** (11.1 wt%, 89 mM) and **BTA (*S*)-Val** (11.5 wt%, 92 mM) in  $\text{C}_6\text{D}_{12}$  at  $25^\circ\text{C}$ . The shape and intensity of the scattering curve of **BTA (*rac*)-Val** is characteristic of the presence of long cylindrical objects. The slope of the scattering intensity is maintained down to the lower measured  $q$  values indicating that objects longer than  $200 \text{ \AA}$  are present. The shape and intensity of the scattering curve of **BTA (*S*)-Val** is characteristic of the presence of small assemblies, corroborating the formation of dimers exclusively (FT-IR data, Fig. S14).

## References.

1. A. Desmarchelier, X. Caumes, M. Raynal, A. Vidal-Ferran, P. W. N. M. van Leeuwen and L. Bouteiller, *J. Am. Chem. Soc.*, 2016, **138**, 4908-4916.
2. S. L. Mayo, B. D. Olafson and I. W. A. Goddard, *J. Phys. Chem.*, 1990, **94**, 8897-8909.
3. H. Sun, *J. Comput. Chem.*, 1994, **15**, 752-768.
4. H. Sun, *Macromolecules*, 1995, **28**, 701-712.
5. S. A. Nose, *Mol. Phys.*, 1984, **52**, 255-268.
6. A. Desmarchelier, M. Raynal, P. Brocorens, N. Vanthuyne and L. Bouteiller, *Chem. Commun.*, 2015, **51**, 7397-7400.
7. A. Desmarchelier, B. Giordano Alvarenga, X. Caumes, L. Dubreucq, C. Troufflard, M. Tessier, N. Vanthuyne, J. Idé, T. Maistriaux, D. Beljonne, P. Brocorens, R. Lazzaroni, M. Raynal and L. Bouteiller, *Soft Matter*, 2016, **12**, 7824-7838.
8. B. Gabriele, M. Attya, A. Fazio, L. Di Donna, P. Plastina and G. Sindona, *Synthesis*, 2009, **11**, 1815-1820.

## Synthesis.

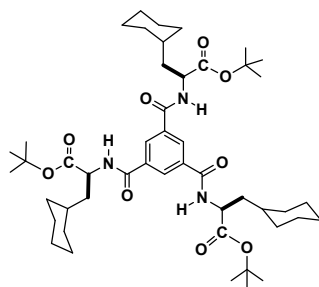


### Tri-N-[(S)-(1-methylene-cyclohexyl)isopropylcarboxymethyl]benzene-1,3,5-tricarboxamide (BTA (S)-Cha<sup>i-Pr</sup>)

**Step1:** (S)-(+)- $\alpha$ -aminocyclohexanepropionic acid hydrate (0.70 g, 4.1 mmol, 1.0 equiv.) in 2-propanol (6 mL) is heated to 70°C, thionyl chloride (0.40 mL, 6.2 mmol, 1.5 equiv.) is added dropwise and the reaction mixture is stirred overnight. After cooling the reaction mixture to room temperature, the crude reaction mixture is dried under reduced pressure. DCM (25 mL) is added and the organic phase is washed with Na<sub>2</sub>CO<sub>3</sub> (10 wt%) and water, dried over MgSO<sub>4</sub> and evaporated under vacuum. The crude thick oil is dissolved in diethyl ether and a 4M solution of HCl in dioxane is added. The precipitate formed is filtrated under vacuum and washed with cold diethyl ether. The colorless solid is dried under vacuum to yield the pure ammonium ester (0.69 g, 2.8 mmol, 68%). <sup>1</sup>H NMR (300 MHz, DMSO-d<sub>6</sub>):  $\delta$  8.46 (br s, 3H), 5.00 (hept,  $J$  = 6.3 Hz, 1H), 3.91 (t,  $J$  = 7.1 Hz, 1H), 1.71-1.57 (m, 8H), 1.46-1.37 (m, 1H), 1.25 (d,  $J$  = 3.0 Hz, 3H), 1.24 (d,  $J$  = 3.0 Hz, 3H), 1.20-1.08 (m, 2H), 0.92-0.81 (m, 2H).

**Step2:** In a flame-dried round-bottom flask under argon atmosphere, benzene-1,3,5-tricarboxylic acid chloride (0.22 g, 0.84 mmol, 1.0 equiv.) is dissolved in dry DCM (30 mL) at room temperature. The ammonium ester (0.69 g, 2.8 mmol, 3.3 equiv.) is then added in one portion, and the resulting mixture is cooled to 0°C with an ice/water bath. Et<sub>3</sub>N (1.0 mL, 7.38 mmol, 8.8 equiv.) is then added dropwise, the reaction is let warm to room temperature and stirred for 48h. Brine is then added to the flask, and the crude mixture is extracted thrice with DCM. The combined organic phases are dried over MgSO<sub>4</sub>, filtered, and the solvent is evaporated under reduced pressure. The resulting solid is taken up as a slurry in a little DCM, and purified on a short column of silica gel (elution: DCM/EtOAc 6:1) to remove salts and impurities ( $R_f$  ~ 0.85-0.9). The product is then purified by column chromatography on silica gel, eluting with DCM/EtOAc 95:5 – 80:20 gradient ( $R_f$  ~ 0.2–0.3) yielding pure BTA (S)-Cha<sup>i-Pr</sup> (0.40 g, 0.50 mmol, 60%) as a crystalline powder. Monocrystals, suitable for X-ray diffraction analysis, were obtained by slowly cooling a warm acetonitrile solution (75°C) of BTA (S)-Cha<sup>i-Pr</sup> (20 mM) to 30°C.

<sup>1</sup>H NMR (300 MHz, acetone-d<sub>6</sub>):  $\delta$  8.53 (s, 3H), 8.28 (d,  $J$  = 7.9 Hz, 3H), 5.06 (hept,  $J$  = 6.3 Hz, 3H), 4.78-4.72 (m, 3H), 1.94–1.56 (m, 25H), 1.38–1.21 (m, 26H), 1.12–0.95 (m, 6H); <sup>13</sup>C{<sup>1</sup>H} NMR (75 MHz, acetone-d<sub>6</sub>):  $\delta$  173.0, 166.6, 135.9, 129.8, 68.9, 51.9, 39.7, 35.0, 34.3, 33.0, 27.1, 27.0, 26.8, 22.1, 22.0; HRMS: Calculated for C<sub>45</sub>H<sub>69</sub>N<sub>3</sub>O<sub>9</sub>Na [M+Na]<sup>+</sup>: 818.4926, found: 818.4924. IR (solid) see Figure S.5.



**BTA (S)-Cha<sup>t-Bu</sup>**

**Tri-N-[(S)-(1-methylene-cyclohexyl)tert-butylcarbonylmethyl]benzene-1,3,5-tricarboxamide (BTA (S)-Cha<sup>t-Bu</sup>)**

**Step1:** The tert-butyl ammonium ester of (S)-(+)- $\alpha$ -aminocyclohexanepropionic acid hydrate is prepared adapting a published procedure.<sup>8</sup> (S)-(+)- $\alpha$ -Aminocyclohexanepropionic acid hydrate (0.48 g, 2.8 mmol, 1.0 equiv.) is suspended in *t*-BuOAc (6.6 mL, 5.80 g, 49.5 mmol, 17.8 equiv.) and concentrated HClO<sub>4</sub> (70%) in water (0.4 mL, 4.5 mmol, 1.6 equiv.) is slowly added at 0°C under Ar atmosphere. The mixture is stirred for 12 h at room temperature. After addition of water (30 mL) and 1 N aqueous HCl (20 mL), the mixture is basified to pH = 9 by addition of 10% aqueous solution of Na<sub>2</sub>CO<sub>3</sub> and extracted thrice with CH<sub>2</sub>Cl<sub>2</sub>. The combined organic phases are dried over MgSO<sub>4</sub> and the solvent is removed under reduced pressure. The crude thick oil obtained is dissolved in diethyl ether and a 4M solution of HCl in dioxane is added. The precipitate formed is filtrated under vacuum and washed with cold diethyl ether. The colorless solid is dried under vacuum to yield the pure ammonium ester (0.32 g, 1.2 mmol, 43%). The synthesis was repeated two times. **<sup>1</sup>H NMR** (300 MHz, DMSO-d<sub>6</sub>):  $\delta$  8.31 (s, 3H), 3.85 (t, *J* = 6.0 Hz, 1H), 1.71-1.57 (m, 7H), 1.45 (s, 9H), 1.24-1.09 (m, 4H), 0.94-0.83 (m, 2H).

**Step2:** In a flame-dried round-bottom flask under argon atmosphere, benzene-1,3,5-tricarboxylic acid chloride (0.19 g, 0.7 mmol, 1.0 equiv.) is dissolved in dry DCM (25 mL) at room temperature. The ammonium ester (0.63 g, 2.4 mmol, 3.3 equiv.) is then added in one portion, and the resulting mixture is cooled to 0°C with an ice/water bath. Et<sub>3</sub>N (0.7 mL, 5.0 mmol, 7.3 equiv.) is then added dropwise, the reaction is let warm to room temperature and stirred for 48h. Brine is then added to the flask, and the crude mixture is extracted thrice with DCM. The combined organic phases are dried over MgSO<sub>4</sub>, filtered, and the solvent is evaporated under reduced pressure. The resulting solid is taken up as a slurry in a little DCM, and purified on a short column of silica gel (elution: DCM/EtOAc 6:1) to remove salts and impurities (*R<sub>f</sub>* ~ 0.85-0.9). The product is then purified by column chromatography on silica gel, eluting with DCM/EtOAc 95:5 – 80:20 gradient (*R<sub>f</sub>* ~ 0.2–0.3), yielding pure **BTA (S)-Cha<sup>t-Bu</sup>** (0.28 g, 0.35 mmol, 50%) as a crystalline powder. Monocrystals, suitable for X-ray diffraction analysis, were obtained by slowly cooling a warm acetonitrile solution (75°C) of **BTA (S)-Cha<sup>t-Bu</sup>** (20 mM) to 30°C.

**<sup>1</sup>H NMR** (300 MHz, DMSO-d<sub>6</sub>):  $\delta$  8.89 (d, *J* = 7.7 Hz, 3H), 8.47 (s, 3H), 4.47–4.41 (m, 3H), 1.76-1.58 (m, 21H), 1.42 (s, 27H), 1.26-1.00 (m, 10H), 0.98-0.76 (m, 8H); **<sup>13</sup>C{<sup>1</sup>H} NMR** (75 MHz, DMSO-d<sub>6</sub>):  $\delta$  171.8, 165.9, 134.5, 129.2, 80.5, 51.1, 37.9, 33.8, 33.0, 31.6, 27.7, 26.0, 25.7, 25.6; **HRMS**: Calculated for C<sub>48</sub>H<sub>75</sub>N<sub>3</sub>O<sub>9</sub>Na [M+Na]<sup>+</sup>: 860.5396, found: 860.5395.

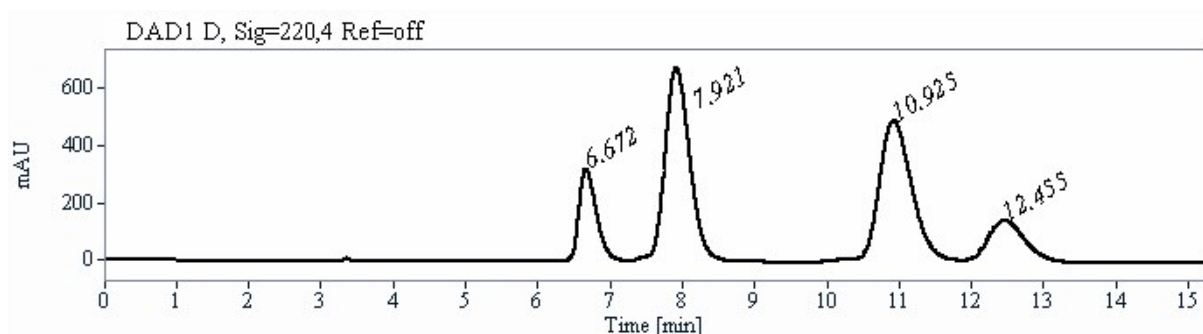
## Isolation of BTA (*S,S,R*)-Val by preparative chiral HPLC

### Conditions:

- Chromatographic conditions: Chiralpak IC (cellulose tris(3,5-dichlorophenylcarbamate) immobilized on silica, 250 x 10 mm), hexane / ethanol (90/10) as mobile phase, flow-rate = 5 mL/min, UV detection at 254 nm.
- Sample preparation: About 500 mg of compound BTA (*rac*)-Val are dissolved in 12 mL of ethanol.
- Injections (stacked): 60 times 200  $\mu$ L, every 10 minutes.

### HPLC traces (BTA (*rac*)-Val):

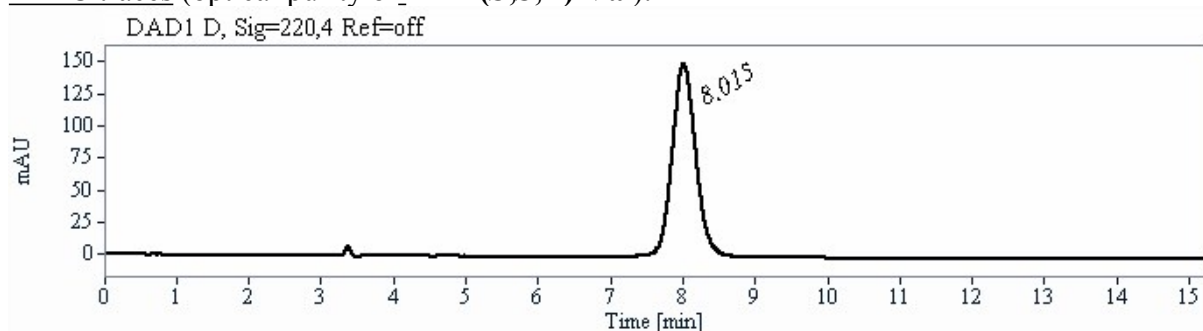
Chiralpak IC (250 x 4.6 mm), hexane / ethanol (90/10) as mobile phase, flow-rate = 1 mL/min, UV detection at 220 nm.



Signal: DAD1 D, Sig=220,4 Ref=off

RT [min]	Area	Area%	Capacity Factor	
6.67	5486	12.73	1.26	BTA ( <i>S</i> )-Val
7.92	16309	37.86	1.68	BTA ( <i>S,S,R</i> )-Val
10.92	15881	36.87	2.70	BTA ( <i>R,R,S</i> )-Val
12.45	5403	12.54	3.22	BTA ( <i>R</i> )-Val
Sum	43078	100.00		

### HPLC traces (optical purity of BTA (*S,S,R*)-Val):



RT [min]	Area	Area%
8.01	3465	100.00
Sum	3465	100.00

The absolute configuration of the second eluted peak was assigned by comparison of the CD spectra of BTA (*S*)-Val and BTA (*S,S,R*)-Val (Fig. S4).

## X-Ray crystal structure determination

Suitable crystals of compounds **BTA (S)-Cha<sup>t-Bu</sup>** and **BTA (S)-Cha<sup>i-Pr</sup>** were grown, mounted and transferred into a cold nitrogen gas stream. Intensity data was collected with a Bruker Kappa-APEX2 system using micro-source Cu-K $\alpha$  radiation. Unit-cell parameters determination, data collection strategy, integration and absorption correction were carried out with the Bruker APEX2 suite of programs. The structures were solved with SHELXT-2014<sup>C1</sup> and refined anisotropically by full-matrix least-squares methods with SHELXL-2014<sup>C1</sup> using the WinGX suite.<sup>C2</sup> Crystal absolute structures were determined by anomalous scattering effects analysis. Chemical absolute configurations were then deduced.<sup>C3</sup> The structures were deposited at the Cambridge Crystallographic Data Centre with numbers CCDC 1491733 et 1491734 and can be obtained free of charge via [www.ccdc.cam.ac.uk](http://www.ccdc.cam.ac.uk).

C1- G. M. Sheldrick, *Acta Cryst. A* **2008**, 64, 112-122.

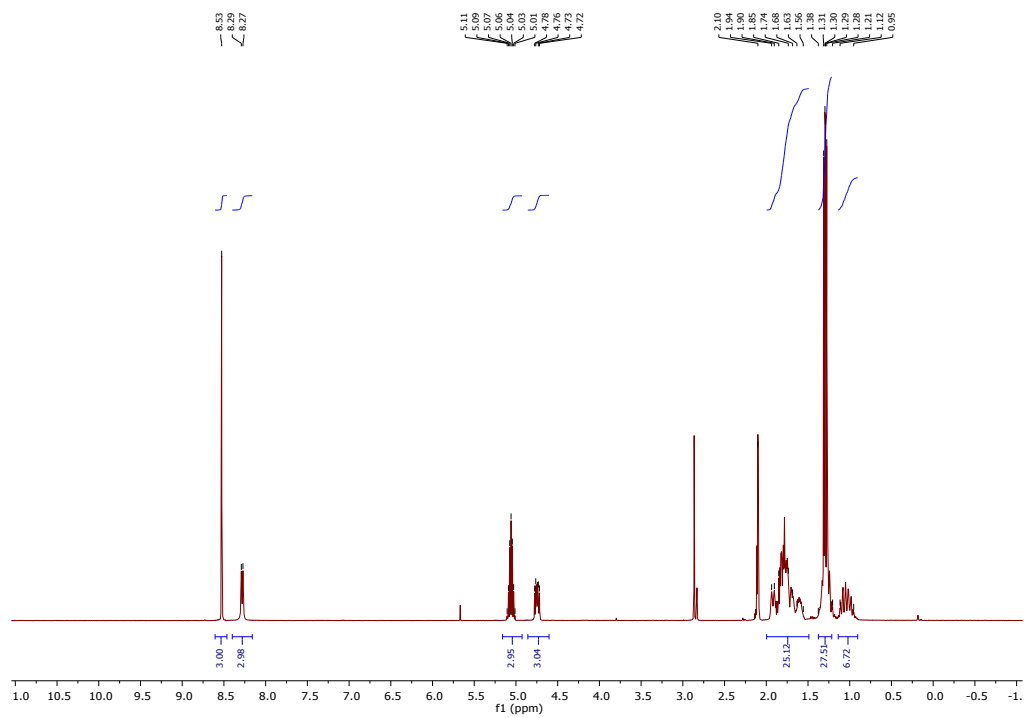
C2- L.J. Farrugia, *J. Appl. Cryst.* **1999**, 32, 837-838.

C3- H.D. Flack, G. Bernadinelli, *Acta Cryst. A* **1999**, 55, 908-915.

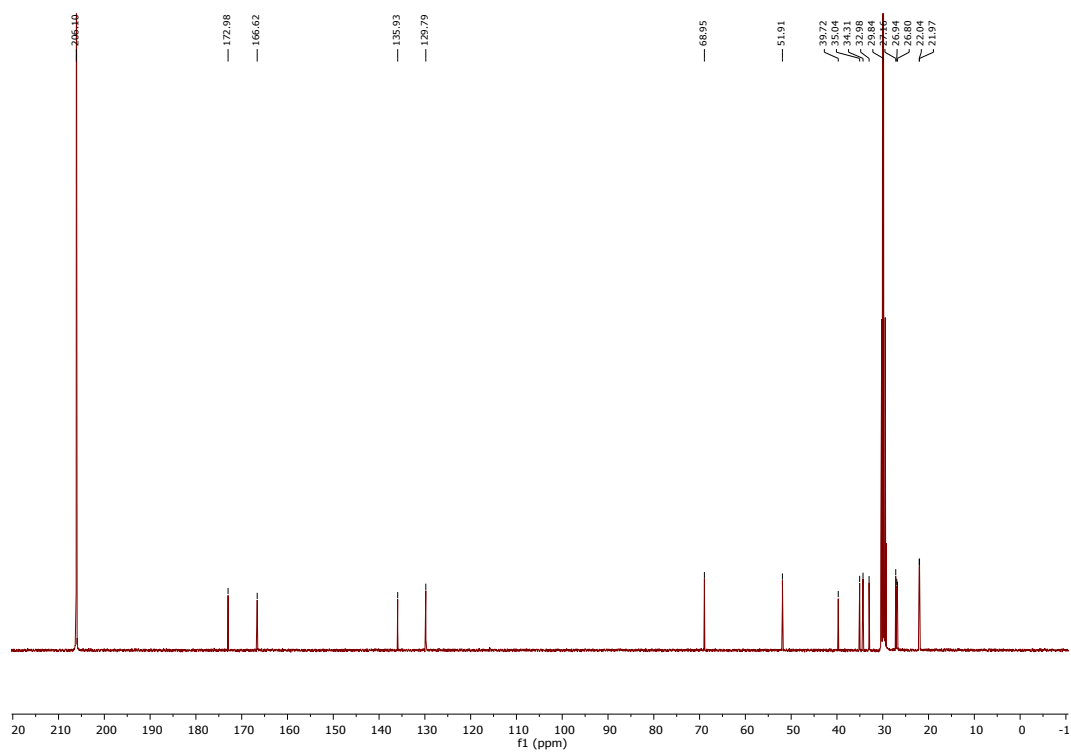
Compound	<b>BTA (S)-Cha<sup>t-Bu</sup></b>		<b>BTA (S)-Cha<sup>i-Pr</sup>. 0.25CH<sub>3</sub>CN·0.5H<sub>2</sub>O</b>	
Empirical formula	C <sub>48</sub> H <sub>75</sub> N <sub>3</sub> O <sub>9</sub>		C <sub>45.5</sub> H <sub>70.75</sub> N <sub>3.25</sub> O <sub>9.5</sub>	
Formula weight	838.11		815.30	
Temperature	200(1) K		200(1) K	
Wavelength	1.54178 Å		1.54178 Å	
Crystal system	Triclinic		Triclinic	
Space group	P 1		P 1	
Unit cell dimensions	a = 12.0223(3) Å	$\alpha = 61.685(2)^\circ$	a = 11.5502(4) Å	$\alpha = 61.491(2)^\circ$
	b = 15.7744(4) Å	$\beta = 76.210(2)^\circ$	b = 15.7414(5) Å	$\beta = 83.352(2)^\circ$
	c = 15.9080(4) Å	$\gamma = 82.022(2)^\circ$	c = 15.8302(5) Å	$\gamma = 79.502(2)^\circ$
Volume	2578.19(12) Å <sup>3</sup>		2485.47(15) Å <sup>3</sup>	
Z	2		2	
Density (calculated)	1.080 g.cm <sup>-3</sup>		1.089 g.cm <sup>-3</sup>	
Absorption coefficient	0.591 mm <sup>-1</sup>		0.611 mm <sup>-1</sup>	
F(000)	912		885	
Crystal size	0.15 x 0.13 x 0.04 mm <sup>3</sup>		0.2 x 0.15 x 0.1 mm <sup>3</sup>	
$\theta$ range for data collection	3.331° to 66.883°		3.179° to 66.651°	
Index ranges	-13<=h<=14, -18<=k<=18, -18<=l<=18		-13<=h<=13, -18<=k<=17, -18<=l<=18	
Reflections collected	34571		43045	
Independent reflections	8533		13780	
R <sub>int</sub>	0.0213		0.0195	
Completeness	99.3%		99.8%	
Max. and min. transmission	0.746 and 0.720		0.752 and 0.700	
Data / restraints / parameters	8533 / 0 / 316		13780 / 93 / 1118	
Goodness-of-fit on F <sup>2</sup>	1.032		1.047	
R1 [I > 2 $\sigma$ (I)]	0.0389		0.0436	
wR2 (all data)	0.1248		0.1234	
Largest difference peak and hole	0.356 and -0.214 e.Å <sup>-3</sup>		0.451 and -0.181 e.Å <sup>-3</sup>	
Absolute structure parameter	-0.03(6)		-0.01(7)	

# BTA (S)-Cha<sup>i</sup>-Pr

<sup>1</sup>H (acetone-d<sub>6</sub>):

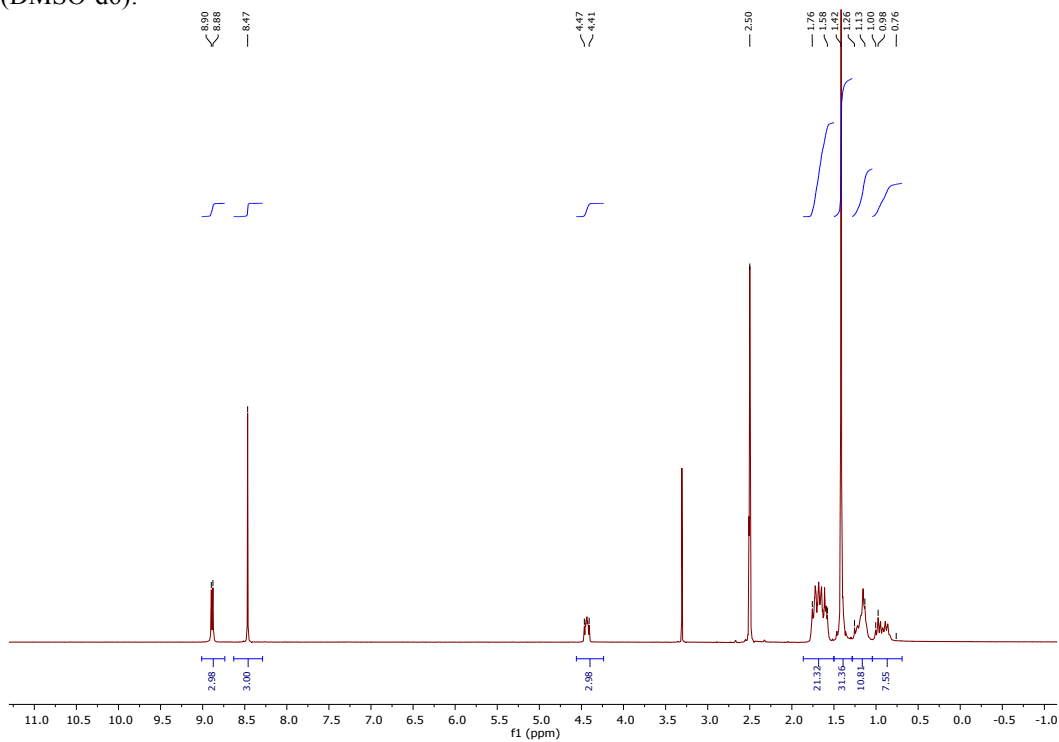


<sup>13</sup>C{<sup>1</sup>H} (acetone-d<sub>6</sub>):



# BTA (S)-Cha<sup>t</sup>-Bu

<sup>1</sup>H (DMSO-d6):



<sup>13</sup>C{<sup>1</sup>H} (DMSO-d6):

